

Research article

Open Access

## Structural analysis of FAD synthetase from *Corynebacterium ammoniagenes*

Susana Frago, Marta Martínez-Júlvez, Ana Serrano and Milagros Medina\*

Address: Departamento de Bioquímica y Biología Molecular y Celular, Facultad de Ciencias and Institute of Biocomputation and Physics of Complex Systems, Universidad de Zaragoza, Zaragoza, Spain

Email: Susana Frago - sfrago@unizar.es; Marta Martínez-Júlvez - mmartine@unizar.es; Ana Serrano - anaserra@unizar.es; Milagros Medina\* - mmedina@unizar.es

\* Corresponding author

Published: 23 September 2008

Received: 7 May 2008

BMC Microbiology 2008, 8:160 doi:10.1186/1471-2180-8-160

Accepted: 23 September 2008

This article is available from: <http://www.biomedcentral.com/1471-2180/8/160>

© 2008 Frago et al; licensee BioMed Central Ltd.

This is an Open Access article distributed under the terms of the Creative Commons Attribution License (<http://creativecommons.org/licenses/by/2.0>), which permits unrestricted use, distribution, and reproduction in any medium, provided the original work is properly cited.

### Abstract

**Background:** The prokaryotic FAD synthetase family – a group of bifunctional enzymes that catalyse riboflavin phosphorylation and FMN adenylylation within a single polypeptide chain- was analysed in terms of sequence and structure.

**Results:** Sequences of nearly 800 prokaryotic species were aligned. Those related with bifunctional FAD synthetase activities showed conservation of several consensus regions and highly conserved residues. A 3D model for the FAD synthetase from *Corynebacterium ammoniagenes* (CaFADS) was generated. This model confirms that the N-terminal and C-terminal domains are related to nucleotidyltransferases and riboflavin kinases, respectively. Models for the interaction of CaFADS with its substrates were also produced, allowing location of all the protein substrates in their putative binding pockets. These include two independent flavin binding sites for each CaFADS activity.

**Conclusion:** For the first time, the putative presence of a flavin binding site for the adenylylation activity, independent from that related with the phosphorylation activity, is shown. Additionally, these models suggest the functional relevance of some residues putatively involved in the catalytic processes. Their relevant roles were analysed by site-directed mutagenesis. A role was confirmed for H28, H31, S164 and T165 in the stabilisation of the P groups and the adenine moiety of ATP and, the P of FMN for the adenylylation. Similarly, T208, N210 and E268 appear critical for accommodation of the P groups of ATP and the ribityl end of RF in the active site for the phosphorylation process. Finally, the C-terminal domain was shown to catalyse the phosphorylation process on its own, but no reaction at all was observed with the individually expressed N-terminal domain.

### Background

The activities of riboflavin (RF) phosphorylation and FMN adenylylation are present among all kingdoms of living organisms. However, whereas eukaryotes use two different enzymes for FMN (flavokinase) and FAD (ade-

nylyltransferase) production [1-6], prokaryotic organisms depend on an enzyme of ~38 kDa, FAD synthetase (Flavin adenine dinucleotide synthetase, FADS), that exhibits both activities [7]. Thus, FADS constitutes a bifunctional prokaryotic protein family of enzymes with both, ATP:RF

5'-phosphotransferase [Riboflavin kinase (RFK) (EC 2.7.1.26) (Flavokinase)] and ATP:FMN-adenylyltransferase [FMN adenylyltransferase (EC 2.7.7.2)] activities [7,8] that catalyses the 5'-phosphorylation of RF to FMN and, subsequently, the adenylylation of FMN to FAD.



The FMN adenylylation reaction of FADS is a reversible process, while phosphorylation of RF appears to be irreversible [9]. Additionally, FADS has been shown to function with a broad variety of RF isoesters, and it is, therefore, widely used in the preparation of FMN and FAD analogues [8,10]. A kinetic mechanism for the steady-state reaction of the FADS from *Corynebacterium ammoniagenes* (*CaFADS*) has been proposed [9], suggesting an order in substrate binding and product release. The FMN intermediate produced by the first reaction appears to be released by the enzyme to later rebind the enzyme as a substrate for FAD production. Both enzyme activities present important differences in their substrate requirements, including concentration dependence, specificity for divalent cations and optimal pH or temperature [7,11,12].

The C-terminal region of FADS (~150 residues) shares considerably sequence similarity with eukaryotic monofunctional RFKs. Likewise, the N-terminal region has been proposed to present remote similarity to nucleotidyltransferases (NTs), suggesting its involvement in the adenylylation process [13]. The structure of bifunctional FADS has only been reported for the *Thermotoga maritima* enzyme (*TmFADS*), both free and in complex with some substrates [14,15]. This structure shows that the enzyme is folded in two domains and it also confirms the presence of one ATP-binding site in each of the domains and a single flavin-binding site [14,15]. So far, neither functional studies of the *TmFADS* nor FADS structures from any other species have been reported.

A sequence analysis of the bifunctional FADS family and an *in silico* structural model for the *CaFADS* are here presented. Based on these data, a preliminary functional analysis of the *CaFADS* has been performed. Several residues are shown to be exclusively involved in either the first or second catalytic event. Additionally, the C- and N-terminal domains have been independently produced and assayed for their activities. The structural information here provided might help to envisage the rational design of selective antimicrobial drugs with the function of inhibiting FMN or FAD production and therefore, the availability in the cell of enzymes depending on these cofactors.

## Methods

### Sequence searches and alignments

The primary structure of *CaFADS* (sp|Q59263|RIBF\_CORAM) was obtained from the UniProtKB/SwissProt database [12]. A SIB-BLAST search of the complete *CaFADS* amino acid sequence was performed at <http://www.expasy.ch/tools/blast/> [16] against the Eukaryota and Bacteria+Archaea subsections of the non-redundant data base UniProt Knowledgebase (Swiss-Prot + TrEMBL). Multiple sequence alignment was generated using the CLUSTAL W algorithm <http://www.ebi.ac.uk/clustalw/> with default parameters [17]. Graphical representation of the multiple sequence alignment was visualised using the WebLogo server <http://weblogo.berkeley.edu> (Figure 1) [18]. The sequence numbering used throughout the paper corresponds to *CaFADS*.

### Prediction of a three-dimensional model for the structure of FAD synthetase from *C. ammoniagenes*

The structural model for *CaFADS* was constructed using homology modelling procedures based on multiple structure-base sequence alignments (including all the proteins in the PDB) as implemented in the Geno3D Web server [19]. This program uses distance geometry, simulated annealing and energy minimisation algorithms to build the protein models. The structural quality of the models was checked using the PROCHECK validation program [20]. The structures of *TmFADS* (1mrz, 1s4m, 1t6x, 1t6y) [14,15] and those of RFKs from *H. sapiens* (1q9s, 1p4m) [21,22] and *S. pombe* (1n06, 1n08) [23] were suitable as templates. Six different combinations of templates were used and three models were generated by each combination.

### Prediction of substrate binding sites

Predictions of putative ATP, Mg<sup>2+</sup> and FMN binding sites of *CaFADS* for FMN adenylylation at the N-terminal domain were carried out by comparing our models with the structures of the nicotinamide mononucleotide adenylyltransferases (NMNAT) in complex with their substrates (Table 1). Similarly, to model ATP, Mg<sup>2+</sup> and RF binding to the C-terminal domain of *CaFADS*, the structures of two RFKs in complex with their substrates (Table 1), as well as the different structures reported for *TmFADS* bound to its different substrates (Table 1), were used. O [24], Spdb-Viewer 3.7 [25] and PyMol 0.99 softwares [26] were used for complex modelling, structural analysis and figures production.

### Cloning and production of *C. ammoniagenes* wild-type and mutated FAD synthetase forms in *E. coli*

Following the Ethical Rules established at the Universidad de Zaragoza, strain DSM 20305 (ATCC 6872) from *C. ammoniagenes* was grown at 30°C in a culture medium containing 0.5% glucose, 0.5% NaCl, 1% tryptone and

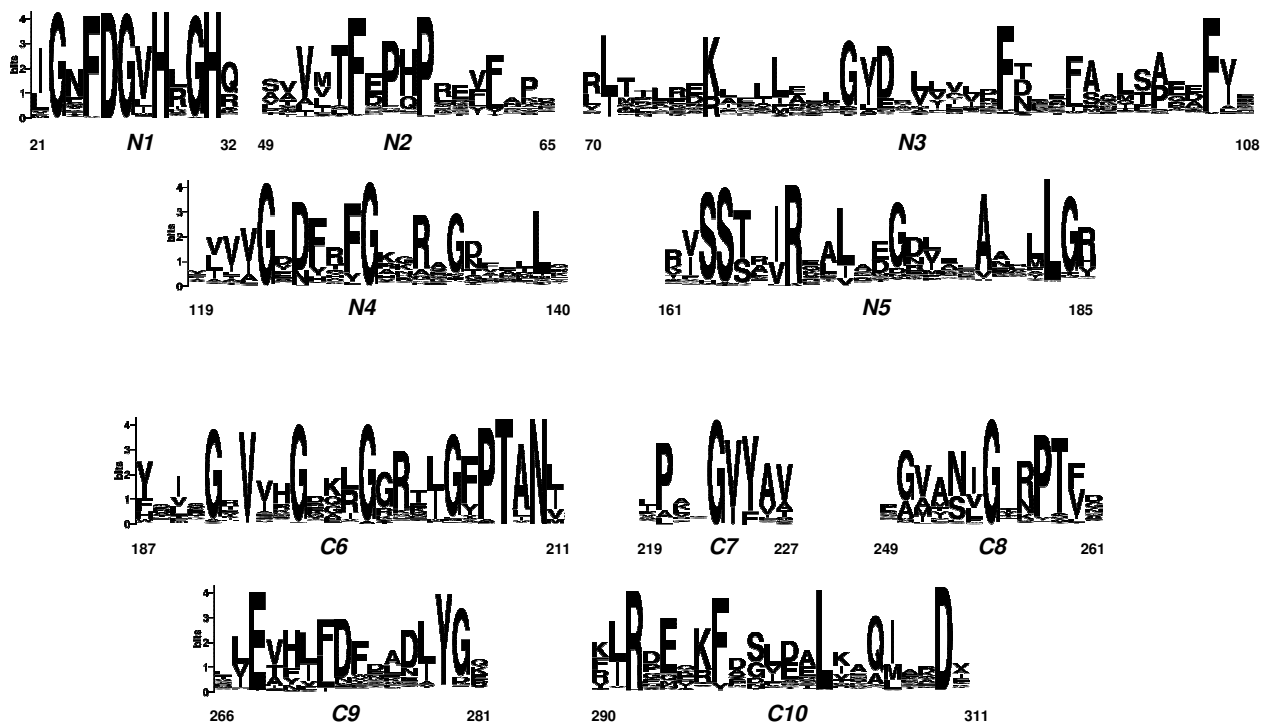


**Figure 1**  
**Sequence logos including the bifunctional FADS family consensus regions and conserved residues.** Numeration of *CaFADS* is used. The data of this logo is based on 500 sequences from the bacteria+archaea alignment of the FADS family. The sequence logo was produced using the WebLogo server <http://weblogo.berkeley.edu> [18].

0.5% yeast extract, pH 7.2–7.4. Genomic DNA was isolated from the cells as previously described [27]. The *CaFADS* encoding sequence was then amplified by the polymerase chain reaction using the forward 5'-GTAAGCCATGGATATTGGTACGGAACAG-3' and reverse 5'-CCATCGATAGCGGATCCGGCATATAC-3' primers, synthesised on the basis of the published nucleotide sequence of the enzyme [12]. The primers incorporate the *NcoI* and *BamHI* sites respectively, and have the transcription start codon GTG replaced with ATG. The amplified 1237 bp DNA fragment was then cloned in the *NcoI/BamHI* sites of the pET-28a(+) expression vector. The resulting recombinant plasmid, PET28a-FADS, was used to transform *E. coli* BL21(DE3) competent cells. The transformants were selected on solid LB/agar medium containing 30 µg/ml kanamycin. The fragment was sequenced to confirm the accuracy of the amplification. Mutations were introduced into the cloned structural gene

encoding the WT *CaFADS* by site-directed mutagenesis. The H28A, H28D, H31A, H31D, R161A, R161D, S164A, S164D, T165A, T165D, T208A, T208D, N210A, N210D, E268A and E268D FADS mutants were generated using the QuikChange mutagenesis kit (Stratagene) in combination with the adequate synthetic oligonucleotides. The gene coding for the individual N-terminal domain (PET28a-Δ(183–338)FADS) was obtained replacing the codon coding for Leu183 in PET28a-FADS with a stop codon, following the methodology above mentioned for production of site-directed mutants. The C-terminal domain was individually cloned (PET28a-Δ(1–182)FADS) using the protocol described for WT *CaFADS* with the forward primer 5'-CCAACTGGGCCATGGGGCGGCAC-3' and the reverse primer above used for the full length protein cloning. The forward primer used to clone the C-terminal domain incorporates the start codon ATG in a *NcoI* site substituting for Leu183. Mutations were ver-

**Table 1: Structures used to model CaFADS and the interaction with its ligands.**

	PDB	SUBSTRATES	(%) IDENTITIES	(%) CONSERVATIVE SUBSTITUTIONS	REFERENCE
<b>FAD synthetases</b>					
<i>T. maritima</i>	1mrz		29.3	40.2	[14]
N-terminal <sup>a</sup>			30.6	39.2	
C-terminal <sup>b</sup>			27.6	41.5	
<i>T. maritima</i> complexed	1s4m	RF	29.3	40.2	[15]
	1t6x	ADP			
	1t6y	FMN, ADP, AMP			
<b>Nucleotidyltransferases<sup>a</sup></b>					
GCT <i>B. subtilis</i>	1coz	CTP	12.4	23.1	[30]
NMNAT <i>M. jannaschii</i>	1f9a	Mg <sup>2+</sup> , ATP	12.9	22.0	[32]
NMNAT <i>H. sapiens</i>	1kku		10.8	18.3	[31]
NMNAT <i>M. thermoautotrophicum</i>	1ej2	NAD <sup>+</sup> , Na <sup>+</sup>	13.0	22.6	[33]
PPAT <i>E. coli</i>	1b6t	dPCoA	13.0	26.3	[34]
	1gn8	ATP, Mn <sup>2+</sup>			[37]
PPAT <i>T. thermophilus</i>	1od6	Ppant	11.3	22.0	[35]
<b>Riboflavin kinases<sup>b</sup></b>					
<i>H. sapiens</i>	1p4m	ADP, Mg <sup>2+</sup> , FMN	25.7	41.4	[21]
	1q9s	ADP, Mg <sup>2+</sup> , FMN			[22]
	1nb0	ADP, Mg <sup>2+</sup>			[21]
<i>S. pombe</i>	1n06	ADP			[23]
	1n07	FMN, ADP	23	38.2	
	1n08	Zn <sup>2+</sup> , ADP			

Parameters derived from the structure-based sequence alignment of the produced CaFADS models over structural databases.

<sup>a</sup> Alignments with the segment 19–186 from CaFADS

<sup>b</sup> Alignments with the segment 187–338 from CaFADS

ified by DNA sequence analysis. WT and mutant FADS proteins were over-expressed in *E. coli*.

#### **Purification of recombinant FADS from *C. ammoniagenes***

*E. coli* cells containing the recombinant pET28a-FADS plasmid (or its mutants) were grown in LB. During the exponential *E. coli* growing phase, FADS was induced by overnight incubation at 37°C with IPTG (1 mM). Cells were harvested by centrifugation and stored at -20°C. In a typical purification, around 25 g of cells (over-expressing recombinant FADS) were thawed, resuspended in 125 ml of cell disruption buffer (50 mM Tris/HCl, pH 8.0, 1 mM EDTA, 12 mM β-mercaptoethanol, 1 μM PMSF) and broken by ultrasonic treatment at 4°C using 16 cycles of 1 min in a DRH UP200 DR Hielsher sonicator. The cell debris was removed by centrifugation at 40000 g during 45 min. The resulting yellow FADS-containing supernatant was fractionated with 45% ammonium sulphate. The mixture was again centrifuged for 45 min at 4000 g and the supernatant was loaded onto a Phenyl-Sepharose High performance (Amersham Biosciences, GE Healthcare) column equilibrated with 50 mM Tris/HCl, pH 8.0, 45% ammonium sulphate. The column was washed with the same buffer containing only 17% ammonium sulphate until most of the yellow colour washed out of the column. The enzyme was eluted using a 17→0% ammo-

nium sulphate reversed-gradient in the same buffer. Fractions of 6–8 ml were collected while the absorbance at 280 nm was recorded. Fractions presenting absorbance at 280 nm were analysed by SDS-PAGE and, those containing the over-expressed FADS were pooled and dialysed against 50 mM Tris/HCl, pH 8.0. After dialysis the protein was loaded onto a DEAE-cellulose (DE52, Whatman, England) column equilibrated with 50 mM Tris/HCl, pH 8.0. The column was washed with the equilibration buffer containing 0.1 M NaCl and subsequently eluted using a 0.1→0.5 M NaCl gradient. Fractions of 5 ml were collected while recording the absorbance at 280 nm and, subsequently analysed by SDS-PAGE. The enzyme was considered pure when a single band of the expected size was observed in SDS-PAGE. Pure FADS fractions were pooled together, dialysed against 50 mM Tris/HCl, pH 8.0 and stored at -20°C.

#### **Measurement of riboflavin kinase and adenylyltransferase activities of FAD synthetase**

Conversion of RF into FMN and, of FMN into FAD were qualitatively assayed by addition of the different FADS variants (final enzyme concentration ~1 μM, calculated using a theoretical ε<sub>280 nm</sub> = 27.8 mM<sup>-1</sup>cm<sup>-1</sup>) to a solution (final volume, 150 μl) containing 50 μM flavin (either RF or FMN), 0.2 mM ATP and either 0.8 mM or 10 mM MgCl<sub>2</sub>, in 50 mM Tris/HCl, pH 8.0. All these chemicals



were obtained from SIGMA and were from the highest purity available. After 30 minutes of incubation at 37°C, the reaction was stopped by boiling the preparations for 5 minutes. Transformation of RF into FMN and FAD, or FMN into FAD, was visualised by resolving the products of the reaction at room temperature and in the dark by TLC on Silica Gel SIL-G-25 (20 cm × 20 cm, thickness 0.25 mm) plates [28]. The moving phase was a solution of butanol:acetic acid:water (12:3:5). Flavin TLC spots were visually examined and scanned by determining their fluorescence under an ultraviolet light. The different flavins move up the plate at different rates due to differences in their partitioning behaviour between the mobile liquid phase and the stationary phase. The weaker intensity of the FAD fluorescence with regard to equivalent amounts of RF or FMN relates with its flavin fluorescence quenching upon stacking of the adenine portion [29]. An additional band, running slightly faster than FMN, is observed in some experiments. The nature of this band is not known, but it is only present in the experiments containing simultaneously FMN and FAD.

## Results and discussion

### Sequence analysis of the FAD synthetase family

No matches for bifunctional FADS sequences were obtained when performing the SIB-BLAST search of the CaFADS sequence on the UniProt Knowledgebase eukaryota subsection. When searching the bacteria+archaea database subsection (2,929,087 sequences searched), the 777 sequences displaying E-values  $\leq 0.009$  were chosen for further analysis. Redundant sequences from the same species presenting sequence identity over 80% were eliminated. The remaining sequences included some proteins noticeably shorter as well as proteins lacking the typical consensus sequences found in FADSs. These sequences (less than 5%), most of them displaying the lowest E-values of the selected sequences, were removed and separately analysed. They could be sorted out into several groups: i) proteins that present only the N-terminal region of FADS, ii) proteins that present only the C-terminal region of FADS, iii) proteins that lack the first conserved motif in the N-terminal region, iv) proteins with a conserved N-terminal region and a C-terminal region that shares no similarity with the bifunctional FADS family, and v) proteins with a conserved C-terminal region and a N-terminal region that shares no similarity with the bifunctional FADS family (in *Rhodococcus sp.* RHA1, the protein N-terminal region is 40% identical to 3,4-dihydroxy-2-butanone-4-phosphate synthase, an enzyme involved in RF biosynthesis). Some of these divergent proteins belong to organisms that also possess a typical prokaryotic FADS sequence.

After the manual refinement, a multiple sequence alignment over the remaining 500 FADS-like sequences, dis-

playing E-values  $\leq 2 \times 10^{-6}$  with CaFADS, was carried out. Only FADSs from the genus *Corynebacterium* displayed sequence identities over 50% with the CaFADS (up to 60% identity in the case of the FADS from *C. efficiens*). However, the multiple alignment pointed out several highly conserved residues and motifs (Figure 1). Motifs 21- $\Phi$ -G- $\Omega$ -F-D-G- $\Phi$ -H- $\Omega$ -G-H- $\Omega$ -32 and 162- $\Phi$ -S-S-[TS]- $\Omega$ -[IV]-R- $\Omega$ - $\Omega$ - $\Phi$ - $\Omega$ - $\Psi$ -G-174 ( $\Phi$ ,  $\Psi$  and  $\Omega$ , denoting hydrophobic, polar and any residue, respectively) (N1 and N5 in Figure 1) corresponded to two consensus sequences in the FADS family that are also conserved in NTs remotely related to FADS (see below). Two additional consensus sequences in between the above mentioned motifs were also observed. They included residues 50- $\Omega$ - $\Phi$ - $\Phi$ - $\Omega$ -F- $\Psi$ -P-[HQ]-P- $\Omega$ -59 and 120- $\Phi$ - $\Phi$ - $\Phi$ -G- $\Omega$ -[DN]-[FYH]- $\Omega$ -[FY]-G- $\Omega$ -129 (N2 and N4 in Figure 1) and, apparently, only the motif 123-G- $\Omega$ - $\Psi$ -125 presents an equivalent in NT sequences (see below). Multiple sequence alignment also showed a number of residues highly conserved, or conservatively substituted, between residues 1 and 186: I71, R77, G85, I86, D87, F94, F98, Y106, V107, A179, L183 and G184 (CaFADS numbering). These residues are mainly included in region N3 and at the end of N5 in Figure 1 and, can be considered as forming additional consensus sequences. Noticeably, only R77 and A179 are conserved in NTs.

The C-terminal region of the bifunctional FADS sequences (residues 187–338) also included several consensus sequences, 191-G- $\Omega$ -V- $\Phi$ - $\Psi$ -G- $\Omega$ - $\Omega$ -G- $\Omega$ - $\Psi$ - $\Phi$ -203, 205-G-[FY]-P-T-[ALIV]-N-210, 223-P- $\Omega$ - $\Omega$ -G-[VI]-[YF]-225, 253- $\Psi$ - $\Phi$ -G- $\Omega$ - $\Psi$ -P-T-[FVI]-260, 267-[LVI]-E- $\Omega$ -[HFYN]- $\Phi$ -[FL]-[DN]-[FWY]- $\Psi$ - $\Phi$ -[DNE]-[LIAV]-Y-[GDN]-280 and 291-[LI]-R- $\Omega$ -[EQMN]- $\Omega$ -[KRT]-[FY]-296, and the highly conserved residues L303 and D310 (see C6–C10 in Figure 1), being all of them also conserved in the sequences of RFKs (see below).

### Structural model of the FAD synthetase from *C. ammoniagenes*

A 3D structural model for the CaFADS has been produced based on the structure of the TmFADS (Figure 2) [14,15]. The low sequence similarity of the N-terminal domain of FADSs with NTs prevented these enzymes to be used as templates (Table 1, Figure 3A) [13], but the sequence similarity found at the C-terminal domain of the FADS family with RFKs from *H. sapiens* [21,22] and *S. pombe* (Table 1, Figure 3B) [23] allowed them to be used as templates. These RFKs were used for the construction of the model in those loops where the X-ray structure of TmFADS did not show experimental information [14,15]. Models for the CaFADS C-terminal domain generated using as templates only the structures of RFKs were consistent with the C-terminal structure reported for TmFADS, indicating that RFKs are a good choice as templates for this FADS family

domain. Stereochemistry and energy analysis of the produced models suggested that the model constructed using the FADS and RFK templates reported in Table 2 (Figure 2A) was adequate to describe the 3D structure of *CaFADS* until structures are provided by experimental methods.

According to the model, the protein folds in two domains. The N-terminal domain (residues 18–186) lacks the first 18 residues of the sequence (not present in the *TmFADS* template), while the C-terminal domain (residues 187–318) lacks the last 20 residues (templates were shorter in sequence or presented very low sequence similarity in those residues) (Figures 2 and 3). The main structural arrangements predicted for the *CaFADS* are present in the structure reported for the *TmFADS* [14,15], but our model also showed the disposition of some loops and a 310-helix at the C-terminal domain that are missed in the *TmFADS* structure. Additionally, the C-terminal domain of *CaFADS* showed an insertion around residue 230 with regard to *TmFADS* and many members of the FADS family.

#### **The kinase domain: the C-terminal domain of *C. ammoniagenes* FAD synthetase**

The C-terminal domain of the *CaFADS* model (residues 187–318) folds in a central six-stranded antiparallel  $\beta$ -barrel stabilised between the single final  $\alpha$ -helix ( $\alpha 7$ ), the two small  $\alpha 5$  and  $\alpha 6$  of the N-terminal domain and several loops (Figure 2A). A short  $3_{10}$ -helix is also predicted in our model between residues G201-L204. This C-terminal domain showed a high sequence identity in the 3D space with the structures of the templates (Figures 3B and 4A, Table 1) and, there is no doubt that it must contribute to ATP,  $Mg^{2+}$  and RF binding to produce FMN. Comparison of this model with the reported *TmFADS* and RFKs structures in complex with their substrates will provide information about *CaFADS* residues involved in substrate binding and catalysis (Figures 3B and 4B). Therefore, it is expected that the  $ADP\cdot Mg^{2+}$ , or  $ATP\cdot Mg^{2+}$ , will be nested at one edge of the  $\beta$ -barrel, between two loops (Figure 4B). The first loop (R195-N210) contains the short  $3_{10}$ -helix and the 207-PT $\Phi$ N-210 consensus sequence conserved in RFKs (Figures 1 and 3B) and, it is proposed to stabilise the P groups (Figure 4B). The structures of RFKs

in complex with  $ADP\cdot Mg^{2+}$  also suggest that T208 and N210 might contribute to metal binding [22,23]. The second loop (E268-Y279) starts with the E268 residue, invariant in FADS and RFK families and proposed to link the terminal OH group of the RF ribityl chain, acting as a catalytic base [21-23]. This loop also includes the D277 and Y279 conserved positions, proposed to stabilise the ATP adenine ring, while V193, K202 and D277 might contribute to stabilise the ribose (Figures 1 and 4B) by similarity with RFKs [21,23]. Comparison of models with *TmFADS* and RFKs complexed with RF or FMN suggests that the isoalloxazine ring must be bound in a pocket formed by the outer surface of the  $\beta$ -barrel ( $\beta 8$ – $\beta 10$ ) and the long terminal  $\alpha 7$  helix. The flavin ring might result stabilised by the hydrophobic environment provided by the consensus region 223-G-V-Y-225 and the conserved F206, F270, F297, L303 and M307 residues, while its hydrophilic portion may be pointing towards the opening of the pocket and stabilised by E295 or K296 [15,21,22]. Other residues apparently not directly involved in flavin binding but contributing to the formation of the bottom and top of the pocket include the consensus region 254-G- $\Omega$ - $\Psi$ -P-T-[FVI]-260 and the highly conserved residues R292 and D310, respectively. These two later residues apparently form a salt bridge that contributes to fix the terminal  $\alpha$ -helix close to the top of the flavin ring cavity (Figure 4B). The ribityl chain would extend towards  $\beta 7$ , interacting as above mentioned with E268 (Figure 4B).

The models for *CaFADS* suggest flexibility in the loops connecting  $\beta 6$ – $\beta 7$  and  $\beta 9$ – $\beta 10$  (Figure 2B). Both of these regions are not solved in the structures reported for the *TmFADS* [14,15]. Flexibility is also observed in regions involved in substrate binding (Figure 4B), in agreement with conformational changes observed in RFKs upon substrate interaction [22]. These conformational changes provide additional interactions, for both the ribityl tail and the isoalloxazine ring and, help to anchor the reactive substrates and the catalytic residues in the most adequate disposition for catalysis [21-23]. This analysis also suggests that despite RFKs and FADSs surely share a similar mechanism in the RF phosphorylation reaction, variations in the structural details for substrate binding and catalysis can be expected.

**Table 2: R.m.s.d. (Å) between the three predicted models for *CaFADS* and the structures used for their production.**

Structure	Model 1	Model 2	Model 3
Model 1	0.00	1.34	1.49
Model 2	1.34	0.00	1.22
Model 3	1.49	1.22	0.00
<i>T. maritima</i> FADS (1mrz)	1.53	1.49	1.44
<i>T. maritima</i> FADS, RF (1s4m)	1.60	1.56	1.39
<i>H. sapiens</i> RFK, ADP, $Mg^{2+}$ , FMN (1p4m)	1.74	1.54	1.25
<i>S. pombe</i> RFK, ADP, $Zn^{2+}$ (1n08)	1.82	1.67	1.60

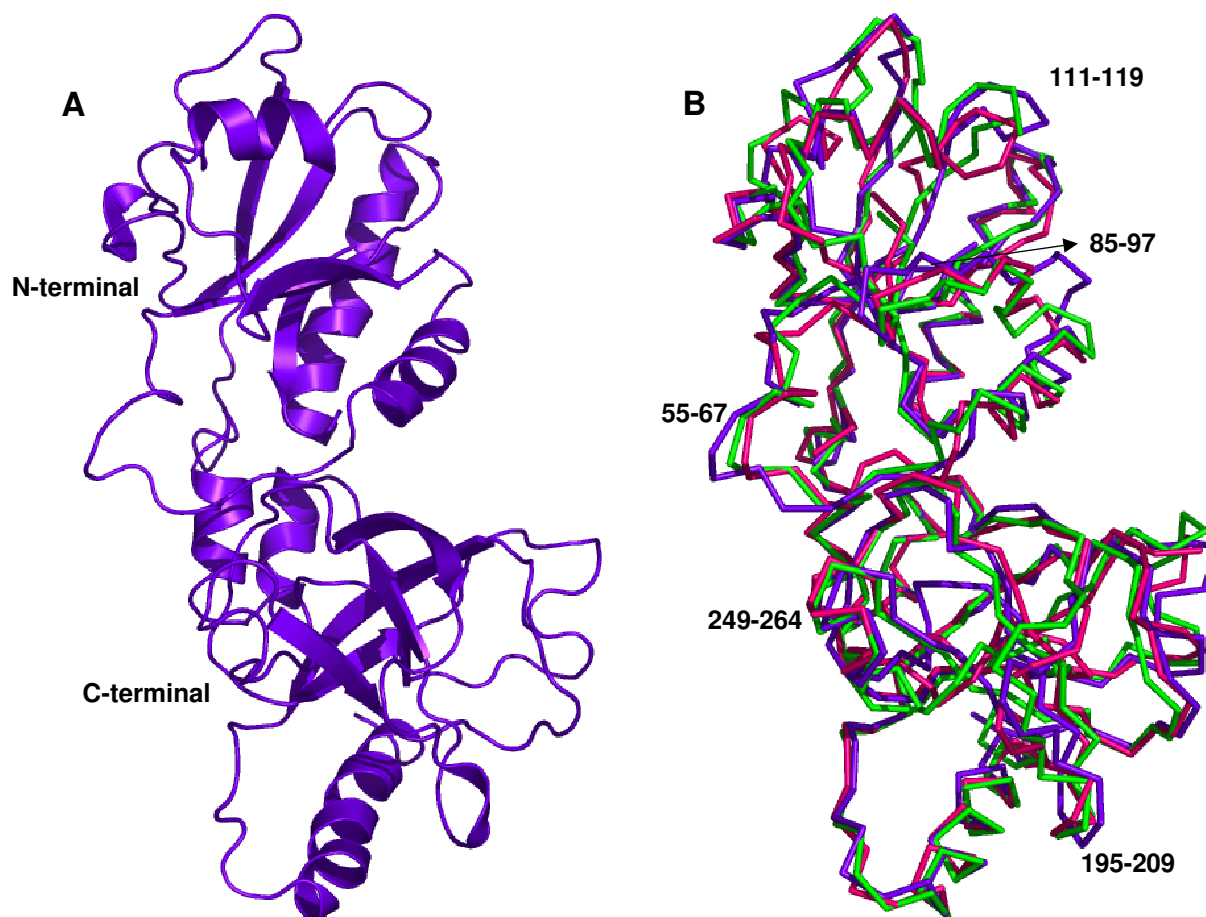


**Figure 2**  
**Predicted structural model for *CaFADS*.** (A) Ribbon representations of the model selected to represent *CaFADS* (Table 2). (B) Superposition of the three models generated in this prediction. Residues involved in putatively high flexible regions are indicated.

#### **The adenylyltransferase domain: the N-terminal domain of *C. ammoniagenes FAD synthetase***

The *CaFADS* N-terminal domain consists of a classical  $\alpha/\beta$  dinucleotide binding domain. Its core is formed by a twisted five-stranded parallel  $\beta$ -sheet flanked by two long and two short  $\alpha$ -helices and the corresponding connecting loops (Figure 5). The end of this domain forms a small subdomain made up of two small  $\alpha$ -helices ( $\alpha 5$  and  $\alpha 6$ ), which are in contact with the C-terminal domain. The *CaFADS* model was compared with the structures reported for several enzymes of the NT  $\alpha/\beta$  phosphodiesterase superfamily (Table 1, Figures 3A and 5A), either free or in complex with their substrates [13-15,30-35]. Members of this family catalyse the transfer of a nucleotide monophosphate moiety, from a nucleotide triphosphate (NTP), onto different substrates. Our *CaFADS* N-terminal model presents an overall folding conserved in

NTs (Figure 5A) that allowed improvement of the sequence alignments and production of putative models for the interaction between this *CaFADS* domain and its substrates (Figures 3A, 5 and 6). The consensus regions 19-32 and 162-174, highly conserved in the FADS and NT families (Figures 1 and 3A), are proposed to be involved in NTP stabilisation in the active site. In our model these motifs include the  $\alpha 1$  helix (H28-V45), placed between  $\beta 1$  and  $\beta 5$ , the E158-S164 loop and some portions of the two terminal antiparallel  $\alpha$ -helices, ( $\alpha 5$  (T165-S172) and  $\alpha 6$  (D175-L183)) (Figure 5). Residues of these consensus regions show a high conservation in primary and 3D structures when comparing the FADS and NT families. Thus, in *CaFADS*: i) main-chain atoms of G22, F24 and D25 might H-bond the  $\alpha$ -P of ATP, ii) H28, G30 and H31 (N-terminal of helix  $\alpha 1$ ) might contribute to stabilise the P groups and adenine moiety of ATP, iii)



**Figure 3** (see previous page)

**Alignments.** (A) Structural alignment of the N-terminal domain of the *CaFADS* model (residues 19–186) with the corresponding regions of *TmFADS* and several NTs. Residues proposed to be involved in particular substrate binding are marked as; ● for phosphate groups, \* ribose or ▲ adenine portions of ATP. ▽ denotes regions where substrates specific for each enzyme have been reported to interact. (B) Structural alignment of the C-terminal domain (residues 187–338) of the *C. ammoniagenes* FADS model with those of *TmFADS* and RFKs from *S. pombe* and *H. sapiens*. Residues proposed to be involved in particular substrate binding are marked as; ● for phosphate groups, \* ribose or ▲ adenine portions of ATP and, △ for the phosphate, ▽ ribityl or ■ isoalloxazine ring portions of RF. Each template is referred to its pdb code according to Table 1. Residues involved in substrate binding in each particular structure are shown in bold case. Consensus sequences are shown below alignment, Φ, Ψ and Ω denoting hydrophobic, polar and any residue, respectively. Secondary structure prediction of *CaFADS*, obtained using the JOY server [36] and visual inspection, is shown above each alignment, with β signifying β-strand residues and α signifying α-helix residues.

the ATP P groups might interact with L34, T38, I162, G174 and the 104–106 and 153–157 regions, iv) the consensus region 162–165 (including the N-terminals of α5) must be involved in stabilisation of the adenine, β-P and γ-P of ATP and, v) the 123–125 consensus motif accommodates the ribose portion of the nucleotide (Figures 3A and 5), as proposed for the equivalent residues in *TmFADS*, glycerol-3 phosphate cytidyltransferase (GCT), phosphopantetheine adenylyltransferase (PPAT) and NMNAT (Figure 3A, 5A) [31,32,34]. The loop formed by residues 156–160 (in red in Figure 5B), although conserved in sequence and structure, shows different orientations and lengths in the different NTs, which probably determines the enzyme specificity for the NTP (Figures 3A and 5A) [30]. The *CaFADS* model also showed several positively charged side-chains highly conserved in the FADS family and structurally situated in positions also occupied by positively charged side-chains in NT structures. These include R161 and R168 (R161 provided by R91 and R22 in PPAT from *E. coli* or *T. thermophilus* and, R168 by K46 in *B. subtilis* GCT or R47 in *M. thermoautotrophicum* NMNAT). Their positions suggest that these side-chains might contribute to stabilise the adenine and P groups of ATP when bound to the active site. It is also worth noting that an important number positions occupied by conserved glycines in the FADS family are also conserved in sequence and structure in NTs and, in many cases, their main-chain atoms directly provide H-bonding to the nucleotide (Figures 1 and 3A).

Flexible regions can be predicted by comparison of the *CaFADS* models (Figure 2B, Table 2). These, including 55–67, 85–97, 111–119 and 127–135, correspond to low similarity regions between NT and FADS families (Figures 2B, 3A and 5A). Structures of NMNAT in complex with NAD<sup>+</sup> [33], and PPAT in complex with dPCoA [34] or Ppant [35], indicate that the binding of the adenylylation substrate, NMN<sup>+</sup> or Ppant moieties, is allocated in the pocket formed by the above mentioned regions. Superposition of these complexes on our *CaFADS* model, followed by fitting and sculpting the FMN molecule along

the nicotinamide nucleotide moiety of NAD<sup>+</sup> in the NMNAT structure, allowed production of putative models for the interaction of the FADS N-terminal domain with its FMN substrate (Figure 6A). In this model, the FMN isoalloxazine ring would be placed in a cavity surrounded by the above mentioned flexible regions. The entrance of this cavity would be flanked by the F54, F62 and D94 hydrophobic side-chains, the consensus region 54-FPHP-58 would fix the position of the ribityl of FMN, while the flavin ring environment would be contributed by hydrophobic interactions with V59, L98, Y106 and F128 (Figure 6A). All these positions are highly conserved in the FADS family, but do not have equivalence in NTs (Figures 1 and 3A). The model suggests that the hydrophobic isoalloxazine portion of the flavin ring might be embedded inside the cavity, while the hydrophilic edge would be partially exposed to the solvent. The size of the cavity makes it difficult to predict the precise location of the isoalloxazine ring. Various possibilities are allowed (Figure 6A) and, final disposition of loops and side-chains would depend on the flavin binding event and conformational changes not predicted in our model. This flavin binding mode could represent a novel flavin binding motif so far not described. Additionally, while sequence motifs N1, N4 and N5 are also conserved in the sequences of eukaryotic FMN adenylyltransferases, residues and regions proposed for flavin binding in the FADS family do not present homologous in the sequences of the monofunctional enzymes (data not shown).

This is the first structural model where a putative binding site for the flavin is suggested at the adenylylation site of FADS, indicating the presence of two independent flavin binding sites in the FADS family. An early hypothetical model for the active site of FADS proposed a single flavin binding site for both activities and two independent ATP binding sites [9]. No structural information of this family of enzymes was reported at that time, but that model accounted for the kinetic mechanism experimentally derived [9]. The 3D structures and models today available for FADS indicate that the phosphorylation and adeny-

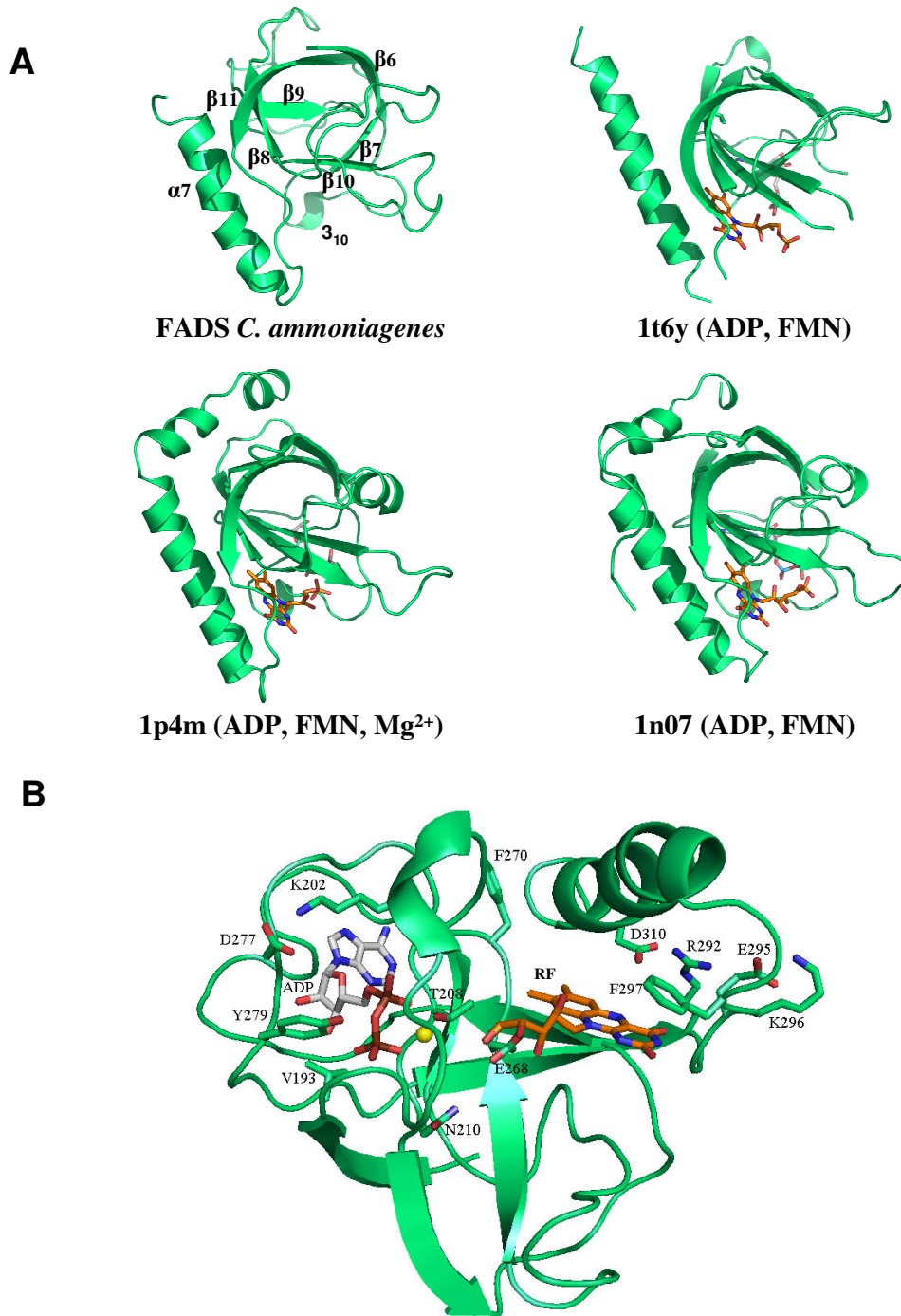


**Figure 4**

**C-terminal domain structure of CaFADS.** (A) Comparison of the structural elements with those found in RFKs. (B) Model for the interaction of ADP-Mg<sup>2+</sup> and RF with the C-terminal domain. Residues putatively involved at the RFK active site, nucleotides and flavins are shown in CPK sticks. Carbon atoms are shown in green, white and orange for protein side-chains, nucleotides and RF, respectively. Mg<sup>2+</sup> ions are shown as yellow balls.

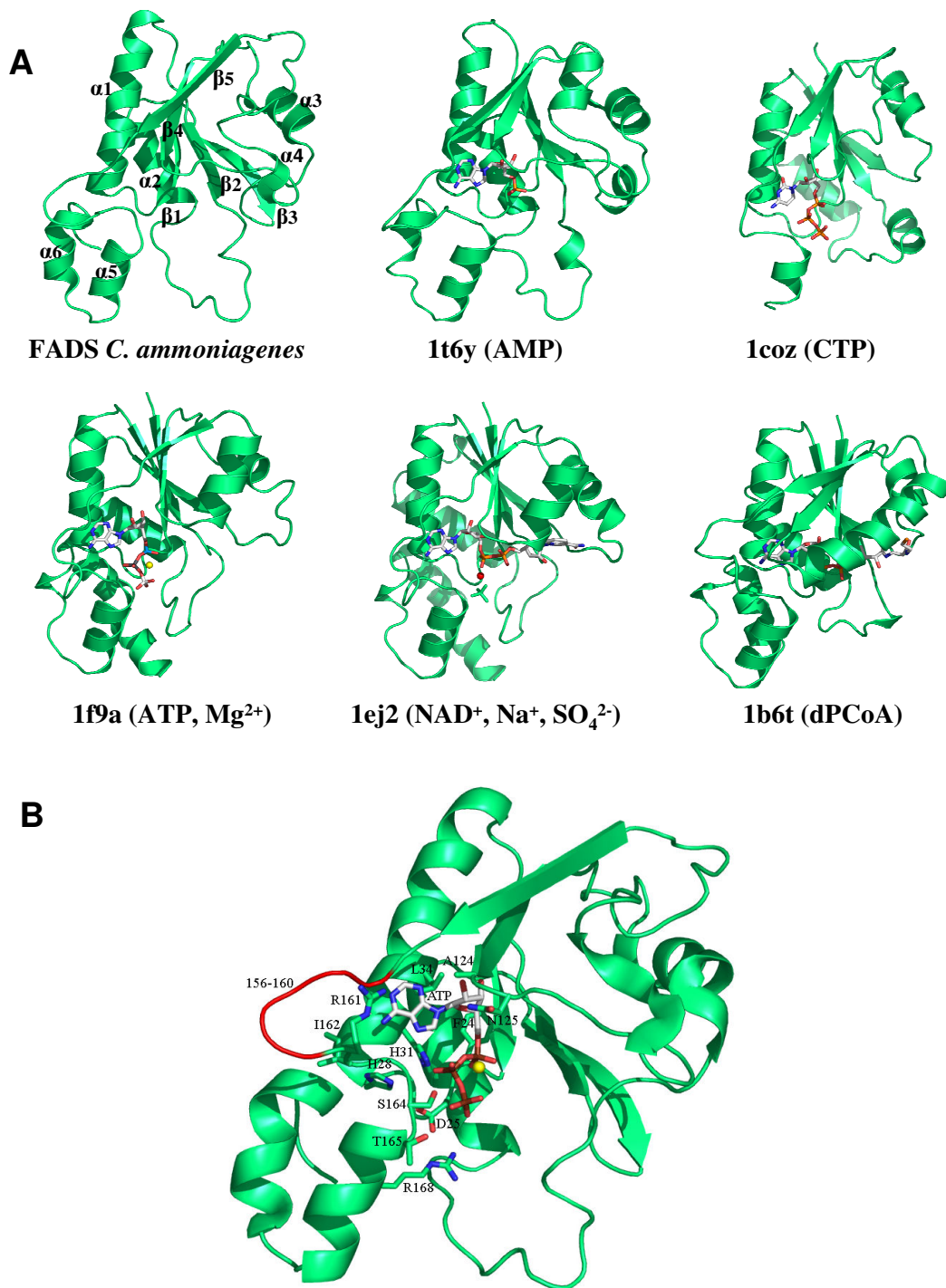


**Figure 5**  
**N-terminal domain structure of CaFADS.** (A) Comparison of the structural elements with those found in NTs. (B) Model for the interaction of ATP-Mg<sup>2+</sup> with the N-terminal domain. Residues putatively involved in the NT activity and ATP binding are drawn as sticks and CPK coloured. Carbon atoms are shown in green and white, for the protein side-chains and nucleotides, respectively. Mg<sup>2+</sup> and Na<sup>+</sup> ions are shown as yellow and red balls, respectively.



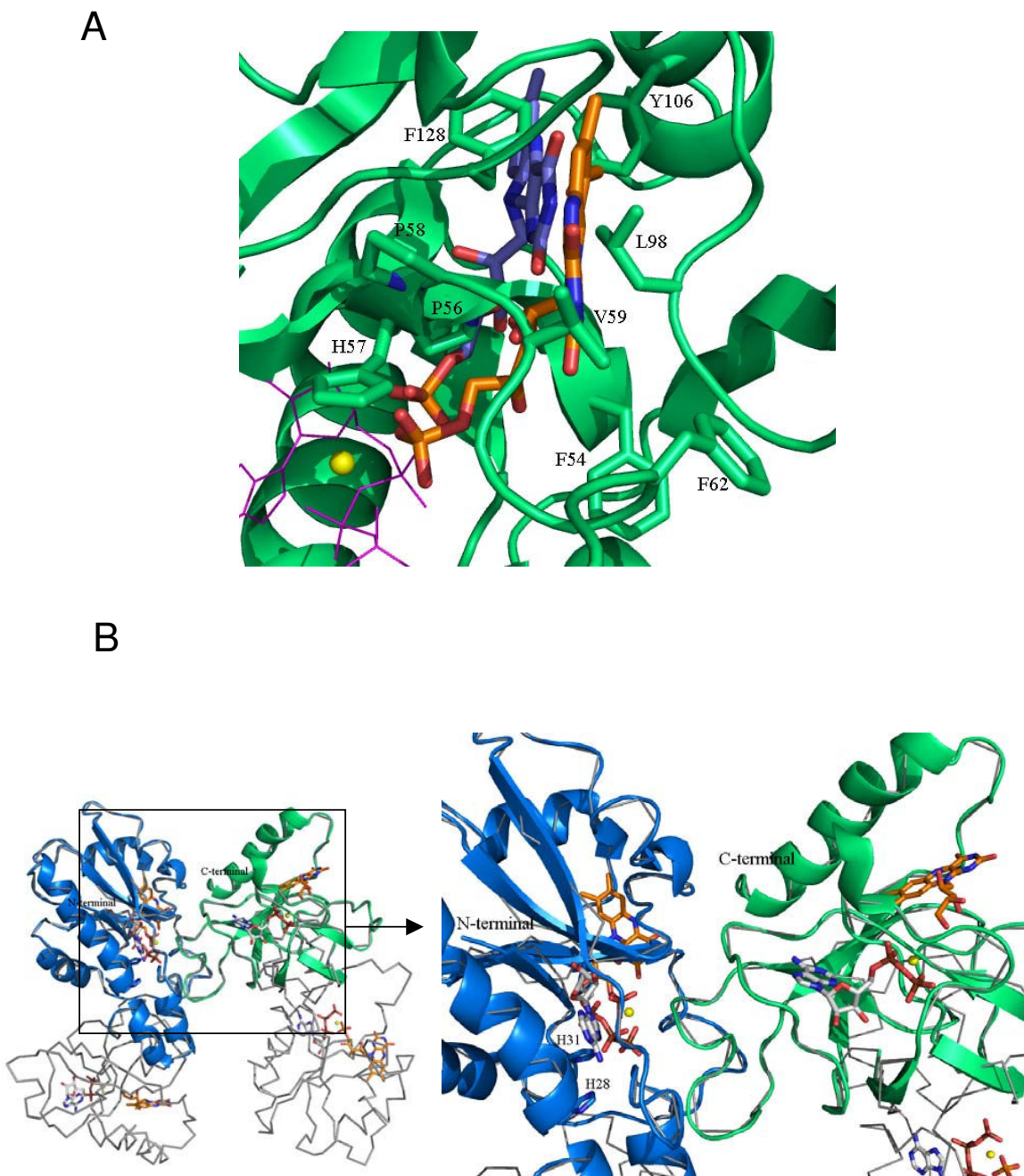


**Figure 6**  
**Localisation of the flavin binding site at the N-terminal domain of CaFADS.** (A) Models for the interaction of FMN with the N-terminal domain. FMN and residues putatively involved in its stabilisation are drawn in sticks and CPK coloured. Two possible conformations for the FMN are indicated (Carbon atoms are in orange and blue, respectively). Positions of ATP and  $Mg^{2+}$  are also indicated as pink lines and a yellow ball, respectively. (B) Model for the interaction between two CaFADS monomers (grey lines), based on the *TmFADS* crystallographic dimeric crystal unit. The C-terminal of monomer 1 is shown in green and the N-terminal of monomer 2 in blue. Position of the RF and FMN substrates, as well as ATP- $Mg^{2+}$ , are indicated at each binding site in CPK. Carbon atoms are shown in white and orange for nucleotides and flavins, respectively. H28 and H31 are shown as sticks.



ylation sites are far away (Figure 6B). This fact is in agreement with experimental observations indicating that the FMN produced in the phosphorylation process was released from the protein, to subsequently rebind to initiate the adenylation process [9]. Superposition of our *CaFADS* model in complex with all its substrates with the dimer reported in the *TmFADS* crystallographic asymmetric unit also indicates that phosphorylation and adenylation active sites from different monomers are far away to share the FMN molecule. However, this dimeric model suggests that the 229–243 loop and the terminal  $\alpha 7$  of the C-terminal domain might contribute to the formation of the ATP and the flavin binding pockets in the adenylation domain (Figure 6B).

### Production of *C. ammoniagenes* FAD synthetase forms

*E. coli* BL21(DE3) cells transformed with the recombinant PET28a-FADS vector produced a high level expression of active *CaFADS*. This *CaFADS* was purified in complex with one of the products of its reaction, FAD, as confirmed by HPLC (data not shown). To remove the FAD a hydrophobic chromatography was required. The sequence and structural analysis suggested the presence of several residues and motifs in *CaFADS* highly conserved in this family of enzymes and potentially involved in the Catalytic sites of the RFK and NT activities. Some of these residues were mutated, namely H28, H31, R161, S164, T165, T208, N210 and E268 to Ala and Asp. These *CaFADS* variants were expressed in *E. coli*, with yields similar to the WT FADS, and were purified to homogeneity following the same protocol. Additionally, plasmids individually expressing the N-terminal and C-terminal *CaFADS* domains were also produced, PET28a- $\Delta(183-338)$ FADS and PET28a- $\Delta(1-182)$ FADS, respectively, and transformed in *E. coli*, showing a level of expression similar to the full length protein.

### *C. ammoniagenes* FAD synthetase residues involved in FMN and FAD production

The ability of the different individual *CaFADS* mutants to catalyse conversion of RF into FMN and of FMN into FAD was analysed by incubating the same amount of each mutant with the substrates of both enzyme activities. Reactions were carried out under two different  $Mg^{2+}$  concentrations; one favouring the RFK activity (0.8 mM) and the other favouring the NT activity (10 mM) [7,11,12]. However, both concentrations produced similar qualitative results under the assayed conditions. The products of the reactions were analysed by TLC (Figure 7).

Replacement of H28 with either Ala or Asp and H31 with Ala prevented conversion of FMN into FAD, confirming their implication in the *CaFADS* NT activity. Both of these His residues belong to a consensus region 27- $\Phi$ -H- $\Omega$ -G-H- $\Omega$ -32 found both in FADS and NT families (Figure 1 and

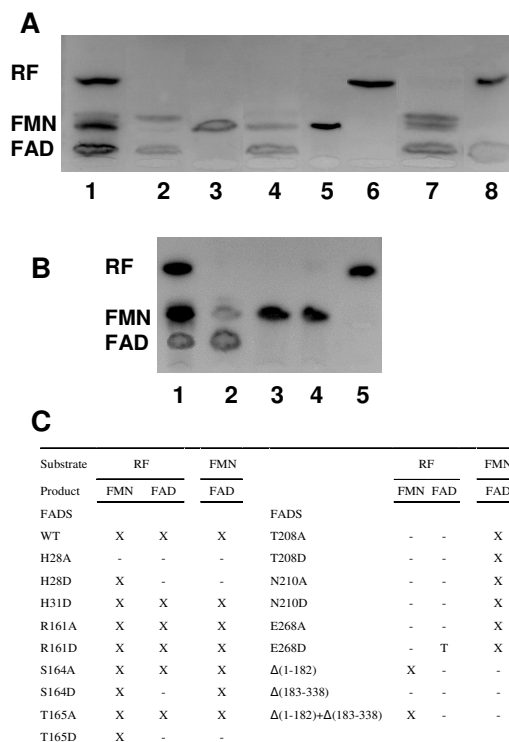


**Figure 7**  
**Resolution by thin layer chromatography of the products of the RFK and the NT activities of selected *CaFADS* variants.** The reaction mixtures contained: (A), 2-WT and 50  $\mu$ M RF, 3-H28D and 50  $\mu$ M RF, 4-R161D and 50  $\mu$ M RF, 5-S164D and 50  $\mu$ M RF, 6-T208A and 50  $\mu$ M RF, 7-T208A and 50  $\mu$ M FMN and 8-E268D and 50  $\mu$ M RF. (B), 2-WT *CaFADS* and 50  $\mu$ M RF, 3-*CaFADS* C-terminal domain and 50  $\mu$ M RF, 4-*CaFADS* C-terminal domain and 50  $\mu$ M FMN and 5-a reaction mixture containing RF incubated in the absence of enzyme. Lanes (1) in (A) and (B) corresponded to a standard solution containing 50  $\mu$ M RF, 50  $\mu$ M FMN and 50  $\mu$ M FAD. All the reaction mixtures contained 0.2 mM ATP and 10 mM  $MgCl_2$  in 50 mM Tris/HCl, pH 8.0. Experiments in (A) were carried out with pure *CaFADS* variants at concentration 1  $\mu$ M, while reaction mixtures in (B) contained crude extracts with the over-expressed *CaFADS* C-terminal domain. (C) Product formation in the assayed samples. X, T and hyphen indicate production, detection of only traces and no production of the corresponding reaction product, respectively.

3A). Therefore, H28 and H31 will surely be major determinants in the stabilisation of the P groups and the adenine moiety of ATP in the reaction transition state in *CaFADS*, in agreement with previous observations in NTs [31,32,34]. Replacement of H28 with Ala also prevented the conversion of RF into FMN, pointing to a possible

influence of the N-terminal domain in the RFK activity. His28 appears situated at the N-terminal of  $\alpha 1$ , in contact with  $\alpha 5$  and  $\alpha 6$ , which, according to our model, will interact with the C-terminal domain from the same polypeptide chain, but also might influence the C-terminal of the second monomer in a putative dimeric structure (Figure 6B). However, it is difficult to envisage how the H28A mutation might affect the phosphorylation reaction with the available information. This will need further structural and biochemical characterisation. Replacement of H31 with Asp produced an enzyme still able to produce FMN and FAD, suggesting that an Asp at this position somewhat replaces the function of the His. Replacements were also introduced in the second major consensus sequence shared by the FADS and the NT families, 162- $\Phi$ SST-165. Replacement of S164 or T165 with Ala produced enzyme forms able to transform RF into FMN and FMN into FAD, while the introduction of a Asp residue at such positions clearly prevented FAD formation. This latter observation was consistent with these residues being involved in the stabilisation at the NT catalytic site of the negatively charged  $\beta$ -P and  $\gamma$ -P of ATP or the ribityl end, as suggested by the above structural analysis (Figures 3A and 5B). Finally, the putative role of the structural disposition of the positive charge of R161 in the stabilisation of the adenine and  $\alpha$ -P and  $\beta$ -P of ATP in the active site was studied by replacement of R161 with either Ala or Asp. The produced FADS mutants were still able to produce FMN and FAD under the assayed conditions, suggesting the positive charge at position of R161 is not playing a critical role in *CaFADS* catalysis.

Taking into account the fact that T208, N210, and E268 are conserved in sequence and structural position in the close environment of the ATP, not only in the FADS family but also in RFKs, and that the terminal oxygen of the ribityl of RF binding sites (Figures 1, 3B and 4), a catalytic role for them in the RF phosphorylation process can be envisaged. These *CaFADS* residues were replaced with Ala or Asp to prove such a role. All these mutations prevented FMN production, but allowed transformation of FMN into FAD, confirming their implication in the RFK activity of FADS. These data are, therefore, in agreement with the proposed structural-based role for T208 and N210 in accommodating the active portion of the ATP molecule, the P groups, and the metal in the catalytic centre (Figure 4B). The lack of FMN and FAD production when replacing E268 with Ala confirms it is a key residue in the *CaFADS* RFK activity. Analysis of the interaction of the *CaFADS* model with FMN (or RF) also indicated that in *CaFADS* E268 side-chain might H-bond to the terminal OH of the ribityl chain of RF (Figure 4B). This Glu is invariant in the FADSs and RFKs families (Figures 1 and 3B). In this later family this residue has been proposed to act as a catalytic base [21-23]. Moreover, the fact that incubation of E268D

with RF did not produce any accumulation of FMN, while traces of FAD were detected, is consistent with the RFK activity taking place at a very slow rate in this mutant, thus avoiding FMN accumulation. This suggests that although the introduced mutation is conservative and the Asp side-chain might still act as a base, its shorter side-chain prevents the optimal organisation of the transition state in the active centre and, therefore, reduces the catalytic efficiency of the RFK activity. Again, this is consistent with this residue not presenting substitutions, even conservative ones, in the analysed proteins. Nevertheless, other explanations might be also possible, as higher catalytic efficiency of NT activity than that of RFK or sensitivity of the TLC analysis. Further work should be done by the analysis of the kinetic parameters for both activities, as well as of the interaction parameters for the different substrates, for all these *CaFADS* mutants to provide additional insights in their specific role in the enzyme catalytic mechanisms.

#### **Activity of the independently produced *C. ammoniagenes* FAD synthetase N- and C-terminal domains**

Crude extracts of the *E. coli* cells expressing the individually cloned N-terminal and C-terminal domains of *CaFADS*,  $\Delta(183-338)$ FADS and  $\Delta(1-182)$ FADS, respectively, were prepared and assayed for NT and RFK activities (Figures 7B, 7C). Analysis of the products of the reaction by TLC concluded that the C-terminal domain,  $\Delta(1-182)$ FADS, was able to qualitatively catalyse the phosphorylation process. However, crude extracts overexpressing the N-terminal domain,  $\Delta(183-338)$ FADS, were not able to catalyse the conversion of FMN into FAD. Extracts containing both domains were mixed and assayed for both reactions. Conversion of RF into FMN was produced in these samples, but they were not able to mimic *CaFADS* in the adenylation process. This is in agreement with a possible C-terminal domain role in contributing to the stabilisation of the flavin and ATP substrates in the corresponding N-terminal domain pockets (Figure 6B).

#### **Conclusion**

A sequence analysis has been carried out in the bifunctional FADS family. An important number of consensus regions and conserved residues have been determined, despite the low sequence identity among members of this family. Sequence divergences found among pathogenic organisms, such as *Mycobacterium* or *Corynebacterium*, and monofunctional eukaryotic enzymes will probably be reflected in structural divergences that might affect the catalytic mechanism, making possible the design of specific antimicrobial drugs. Models have been proposed, not only for the *CaFADS* structure, but also for the complexes formed with all its substrates. This includes the interaction with the FMN substrate at the adenylation site, in a

region not previously reported as involved in the enzyme activity and, in a pocket that might constitute a novel flavin binding motif. As expected, these models supported that the N-terminal presents similar folding to NTs and is involved in the adenylation of FMN, whereas the C-terminal is similar to RFKs and responsible for the phosphorylation. Models of CaFADS allowed identification of several residues putatively involved in the catalysis. Site-directed mutagenesis on some of these residues confirmed their participation in substrate stabilisation and/or the catalytic mechanism. The particular behaviour of some of these mutants and of the independently expressed NT and RFK domains suggests one of the domains might influence the activity in the other one. This study sheds important and new information on the structural mechanism of substrate recognition and catalysis while waiting for the experimental structure of the CaFADS and provides a platform for future investigations into the mechanism of enzymes of the bifunctional FADS family.

#### Authors' contributions

SF carried out the sequence alignment, contributed to production and analysis of the properties of WT FADS and some its mutants and drafted the manuscript. MM-J carried out the production of the three-dimensional FADS model structures free and in complex with ligands. AS participated in the production of the different FADS variants and in its characterisation. MM conceived of the study, and participated in its design and coordination, in the modelling of the three-dimensional structures and drafted the manuscript. All authors read and approved the final manuscript.

#### Acknowledgements

This work has been supported by the Spanish Ministry of Sciences (Grant BIO2007-65890-C02-01 to M.M.).

#### References

- Barile M, Brizio C, Valenti D, De Virgilio C, Passarella S: **The riboflavin/FAD cycle in rat liver mitochondria.** *Eur J Biochem* 2000, **267(15)**:4888-4900.
- McCormick DB, Oka M, Bowers-Komro DM, Yamada Y, Hartman HA: **Purification and properties of FAD synthetase from liver.** *Methods Enzymol* 1997, **280**:407-413.
- Oka M, McCormick DB: **Complete purification and general characterization of FAD synthetase from rat liver.** *J Biol Chem* 1987, **262(15)**:7418-7422.
- Merrill AH Jr, McCormick DB: **Affinity chromatographic purification and properties of flavokinase (ATP:riboflavin 5'-phosphotransferase) from rat liver.** *J Biol Chem* 1980, **255(4)**:1335-1338.
- Brizio C, Galluccio M, Wait R, Torchetti EM, Bafunno V, Accardi R, Gianazza E, Indiveri C, Barile M: **Over-expression in Escherichia coli and characterization of two recombinant isoforms of human FAD synthetase.** *Biochem Biophys Res Commun* 2006, **344(3)**:1008-1016.
- Galluccio M, Brizio C, Torchetti EM, Ferranti P, Gianazza E, Indiveri C, Barile M: **Over-expression in Escherichia coli, purification and characterization of isoform 2 of human FAD synthetase.** *Protein Expr Purif* 2007, **52(1)**:175-181.
- Manstein DJ, Pai EF: **Purification and characterization of FAD synthetase from Brevibacterium ammoniagenes.** *J Biol Chem* 1986, **261(34)**:16169-16173.
- Grill S, Busenbender S, Pfeiffer M, Kohler U, Mack M: **The bifunctional flavokinase/flavin adenine dinucleotide synthetase from Streptomyces davawensis produces inactive flavin cofactors and is not involved in resistance to the antibiotic roseoflavin.** *J Bacteriol* 2008, **190(5)**:1546-1553.
- Efimov I, Kuusk V, Zhang X, McIntire WS: **Proposed steady-state kinetic mechanism for Corynebacterium ammoniagenes FAD synthetase produced by Escherichia coli.** *Biochemistry* 1998, **37(27)**:9716-9723.
- Murthy YV, Massey V: **Syntheses and applications of flavin analogs as active site probes for flavoproteins.** *Methods Enzymol* 1997, **280**:436-460.
- Hagihara T, Fujio T, Aisaka K: **Cloning of FAD synthetase gene from Corynebacterium ammoniagenes and its application to FAD and FMN production.** *Appl Microbiol Biotechnol* 1995, **42(5)**:724-729.
- Nakagawa S, Igarashi A, Ohta T, Hagihara T, Fujio T, Aisaka K: **Nucleotide sequence of the FAD synthetase gene from Corynebacterium ammoniagenes and its expression in Escherichia coli.** *Biosci Biotechnol Biochem* 1995, **59(4)**:694-702.
- Krupa A, Sandhya K, Srinivasan N, Jonnalagadda S: **A conserved domain in prokaryotic bifunctional FAD synthetases can potentially catalyze nucleotide transfer.** *Trends Biochem Sci* 2003, **28(1)**:9-12.
- Wang W, Kim R, Jancarik J, Yokota H, Kim SH: **Crystal structure of a flavin-binding protein from Thermotoga maritima.** *Proteins* 2003, **52(4)**:633-635.
- Wang W, Kim R, Yokota H, Kim SH: **Crystal structure of flavin binding to FAD synthetase of Thermotoga maritima.** *Proteins* 2005, **58(1)**:246-248.
- Altschul SF, Madden TL, Schaffer AA, Zhang J, Zhang Z, Miller W, Lipman DJ: **Gapped BLAST and PSI-BLAST: a new generation of protein database search programs.** *Nucleic Acids Res* 1997, **25(17)**:3389-3402.
- Thompson JD, Higgins DG, Gibson TJ: **CLUSTAL W: improving the sensitivity of progressive multiple sequence alignment through sequence weighting, position-specific gap penalties and weight matrix choice.** *Nucleic Acids Res* 1994, **22(22)**:4673-4680.
- Crooks GE, Hon G, Chandonia JM, Brenner SE: **WebLogo: a sequence logo generator.** *Genome Res* 2004, **14(6)**:1188-1190.
- Combet C, Jambon M, Deleage G, Geourjon C: **Geno3D: automatic comparative molecular modelling of protein.** *Bioinformatics* 2002, **18(1)**:213-214.
- Laskowski RA, MacArthur MW, Moss DS, Thornton JM: **PROCHECK: a program to check the stereochemical quality of protein structures.** *J Appl Cryst* 1993, **26**:283-291.
- Karthikeyan S, Zhou Q, Mseeh F, Grishin NV, Osterman AL, Zhang H: **Crystal structure of human riboflavin kinase reveals a beta barrel fold and a novel active site arch.** *Structure* 2003, **11(3)**:265-273.
- Karthikeyan S, Zhou Q, Osterman AL, Zhang H: **Ligand binding-induced conformational changes in riboflavin kinase: structural basis for the ordered mechanism.** *Biochemistry* 2003, **42(43)**:12532-12538.
- Bauer S, Kemter K, Bacher A, Huber R, Fischer M, Steinbacher S: **Crystal structure of Schizosaccharomyces pombe riboflavin kinase reveals a novel ATP and riboflavin-binding fold.** *J Mol Biol* 2003, **326(5)**:1463-1473.
- Jones TA, Zou JY, Cowan SW, Kjeldgaard M: **Improved methods for building protein models in electron density maps and the location of errors in these models.** *Acta Crystallogr A* 1991, **47(Pt 2)**:110-119.
- Guex N, Peitsch MC: **SWISS-MODEL and the Swiss-PdbViewer: an environment for comparative protein modeling.** *Electrophoresis* 1997, **18(15)**:2714-2723.
- Delano WL: **They PyMOL molecular graphics system.** 2002 [<http://www.pymol.org>]. DeLano Scientific, San Carlos, CA, USA
- Pospiech A, Neumann B: **A versatile quick-prep of genomic DNA from Gram-positive bacteria.** *Trends in Genetics* 1995, **11(6)**:217-218.
- Bauer K, Gros L, Sauer W: **Thin Layer Chromatography: An Introduction.** Germany: Hüthig Verlag; 1991.

29. Berg PAW van den, Feenstra KA, Mark AE, Berendsen HJC, Visser AJVG: **Dynamic conformations of flavin adenine dinucleotide: Simulated molecular dynamics of the flavin cofactor related to the time-resolved fluorescence characteristics.** *J Phys Chem B* 2002, **106(34)**:8858-8869.
30. Weber CH, Park YS, Sanker S, Kent C, Ludwig ML: **A prototypical cytidyltransferase: CTP:glycerol-3-phosphate cytidyltransferase from *Bacillus subtilis*.** *Structure* 1999, **7(9)**:1113-1124.
31. Garavaglia S, D'Angelo I, Emanuelli M, Carnevali F, Pierella F, Magni G, Rizzi M: **Structure of human NMN adenylyltransferase. A key nuclear enzyme for NAD<sup>+</sup> homeostasis.** *J Biol Chem* 2002, **277(10)**:8524-8530.
32. D'Angelo I, Raffaelli N, Dabusti V, Lorenzi T, Magni G, Rizzi M: **Structure of nicotinamide mononucleotide adenylyltransferase: a key enzyme in NAD<sup>+</sup> biosynthesis.** *Structure* 2000, **8(9)**:993-1004.
33. Saridakis V, Christendat D, Kimber MS, Dharamsi A, Edwards AM, Pai EF: **Insights into ligand binding and catalysis of a central step in NAD<sup>+</sup> synthesis: structures of *Methanobacterium thermoautotrophicum* NMN adenylyltransferase complexes.** *J Biol Chem* 2001, **276(10)**:7225-7232.
34. Izard T, Geerlof A: **The crystal structure of a novel bacterial adenylyltransferase reveals half of sites reactivity.** *Embo J* 1999, **18(8)**:2021-2030.
35. Takahashi H, Inagaki E, Fujimoto Y, Kuroishi C, Nodake Y, Nakamura Y, Arisaka F, Yutani K, Kuramitsu S, Yokoyama S, et al.: **Structure and implications for the thermal stability of phosphopantetheine adenylyltransferase from *Thermus thermophilus*.** *Acta Crystallogr D Biol Crystallogr* 2004, **60(Pt 1)**:97-104.
36. Mizuguchi KDC, Blundell TL, Johnson MS, Overington JP: **JOY: protein sequence-structure representation and analysis.** *Bioinformatics* 1998, **14**:617-623.
37. Izard T: **The crystal structures of phosphopantetheine adenylyltransferase with bound substrates reveal the enzyme's catalytic mechanism.** *J Mol Biol* 2002, **315(4)**:487-495.

Publish with **BioMed Central** and every scientist can read your work free of charge

"BioMed Central will be the most significant development for disseminating the results of biomedical research in our lifetime."

Sir Paul Nurse, Cancer Research UK

Your research papers will be:

- available free of charge to the entire biomedical community
- peer reviewed and published immediately upon acceptance
- cited in PubMed and archived on PubMed Central
- yours — you keep the copyright

Submit your manuscript here:  
[http://www.biomedcentral.com/info/publishing\\_adv.asp](http://www.biomedcentral.com/info/publishing_adv.asp)

